ISSN 1062-8738, Bulletin of the Russian Academy of Sciences: Physics, 2024, Vol. 88, No. 8, pp. 1177–1184. © Pleiades Publishing, Ltd., 2024.

Study of the Structure of the ^{9}Be Nucleus in the Alpha-Cluster Model by the Method of Hyperspherical Functions

A. S. Bazhin[a, b, *] and V. V. Samarin[a, b]

[a] *Joint Institute for Nuclear Research, Dubna, Moscow oblast, 141980 Russia*

[b] *Dubna State University, Dubna, Moscow oblast, 141982 Russia*

**e-mail: vichshizik@gmail.com*

Received March 15, 2024; revised March 24, 2024; accepted April 29, 2024

Abstract—The energy and the squared modulus of the wave function of the ground state of the ^{9}Be nucleus as a system of two alpha-clusters and an outer neutron were calculated using hyperspherical functions. A system of hyperradial equations was solved using cubic splines. The charge distribution and the root-mean-square charge radius for the ^{9}Be nucleus were calculated and were found to agree with the experimental data.

DOI: 10.1134/S1062873824707281

INTRODUCTION

It is known that a number of light nuclei can be represented as consisting of alpha-particles (alpha-clusters) and outer (valence) nucleons [1, 2]. The structure of the ^{9}Be and ^{10}Be nuclei as systems consisting of two α-clusters and one neutron ($2\alpha + n$) or two neutrons ($2\alpha + 2n$), respectively, was considered previously [3, 4] using Feynman path integrals. It was shown that the most probable configuration of the ^{9}Be nucleus is the configuration of a nuclear "molecule" with a neutron between α-particles. Easy to implement using parallel calculations, the method of Feynman path integrals allows one to obtain the probability density of a system of several interacting particles in numerical form (in the form of multidimensional tables). This makes it inconvenient to perform averaging over possible particle positions, in particular, when calculating charge distributions and the root-mean-square charge radius. Therefore, in this work, the wave function of the ground state of the three-body system ^{9}Be($\alpha + n + \alpha$) was found using an expansion in hyperspherical functions [5]. The main mathematical task of the method of hyperspherical functions is the numerical solution of a system of hyperspherical equations for functions that are coefficients of expansion in hyperspherical harmonics. In this work, we solved this problem using the cubic spline method [6]. This method allows one to reduce the number of radial grid nodes and find the values of functions between nodes using smooth interpolation, ensuring continuity of the function together with its first and second derivatives. The potential of interaction of α-particles was chosen in the form of a modified potential describing *s*-scattering of low-energy α-particles. The interaction of the neutron with an α-particle was described using the pseudopotential proposed previously [4]. The calculated charge distributions and root-mean-square charge radius agreed with experimental data.

METHOD OF HYPERSPHERICAL FUNCTIONS FOR A THREE-BODY SYSTEM

The Hamiltonian of a system consisting of two α-clusters and a neutron with masses m_α and m_n, respectively, in the center-of-mass system and using Jacobi vectors

$$\vec{R} = \vec{r}_{\alpha 2} - \vec{r}_{\alpha 1}, \quad \vec{r} = \vec{r}_n - \frac{\vec{r}_{\alpha 1} + \vec{r}_{\alpha 2}}{2}, \tag{1}$$

has the form

$$\hat{H} = -\frac{\hbar^2}{2M}\Delta_{\vec{R}} - \frac{\hbar^2}{2\mu}\Delta_{\vec{r}} + V_{\alpha-\alpha}(R) + V_{\alpha-n}(r_1) + V_{\alpha-n}(r_2), \tag{2}$$

where

$$\frac{1}{M} = \frac{1}{m_\alpha} + \frac{1}{m_\alpha}; \quad M = \frac{m_\alpha}{2}; \quad \frac{1}{\mu} = \frac{1}{m_n} + \frac{1}{2m_\alpha}; \quad \mu = \frac{2m_\alpha m_n}{2m_\alpha + m_n}; \tag{3}$$

and $V_{\alpha-\alpha}$ and $V_{\alpha-n}$ are the potential energies of interaction, respectively, of α-particles with each other and an α-particle with the neutron;

$$r_1 = |\vec{r}_n - \vec{r}_{\alpha 1}| = \left|\vec{r} - \frac{1}{2}\vec{R}\right|, \quad r_2 = |\vec{r}_n - \vec{r}_{\alpha 2}| = \left|\vec{r} + \frac{1}{2}\vec{R}\right|. \tag{4}$$

The Schrödinger equation with Hamiltonian (2) for the system in Jacobi vectors has the form

$$-\frac{\hbar^2}{2M}\Delta_{\vec{R}}\Psi - \frac{\hbar^2}{2\mu}\Delta_{\vec{r}}\Psi + \left[V_{12}(R) + V_{13}(\rho_1) + V_{23}(\rho_2)\right]\Psi = E\Psi. \quad (5)$$

After transformation to normalized Jacobi coordinates using quantities (3),

$$\vec{x} = \vec{R}\sqrt{\frac{1}{m_0 x_0^2}}\sqrt{\frac{m_\alpha}{2}}, \qquad \vec{y} = \vec{r}\sqrt{\frac{1}{m_0 x_0^2}}\sqrt{\frac{2m_\alpha m_n}{2m_\alpha + m_n}}. \quad (6)$$

Schrödinger equation (5) for the system takes the simple form

$$-\Delta_{\vec{x}}\Psi - \Delta_{\vec{y}}\Psi + 2b_0\left[\tilde{V}_{12}(R) + \tilde{V}_{13}(\rho_1) + \tilde{V}_{23}(\rho_2)\right]\Psi = 2b_0\tilde{E}\Psi, \quad (7)$$

where $b_0 = m_0 x_0^2 \varepsilon_0/\hbar^2 \approx 0.02392$, $m_0 = 1$ amu, $x_0 = 1$ fm, $\varepsilon_0 = 1$ MeV, $\tilde{E} = E/\varepsilon_0$, and $\tilde{V}(\rho) = V(\rho)/\varepsilon_0$.

The wave function Ψ of the system in the six-dimensional space of Jacobi vectors $(\vec{x}, \vec{y})$ is represented in a form that depends on the hyperradius $\rho = \sqrt{x^2 + y^2}$; four angles θ_x, φ_x, θ_y, and φ_y of the unit vectors $(\hat{\vec{x}}, \hat{\vec{y}})$ in the directions of normalized Jacobi vectors $(\vec{x}, \vec{y})$; and the fifth angle α determined by the ratio of the lengths of these vectors,

$$x = \rho\cos\alpha, \quad y = \rho\sin\alpha. \quad (8)$$

The solution to Eq. (7) is presented in the form of an expansion in known hyperspherical functions depending on the angles $\Omega = (\alpha, \theta_x, \varphi_x, \theta_y, \varphi_y)$ and the quantum numbers L (total momentum), l_x and l_y (orbital momenta of the relative motion of the pair of α-clusters and the motion of the neutron relative to the center of mass of the pair), and the hypermomentum K [5]. In the ground state of the ^{9}Be nucleus, the total momentum is zero, $L = 0$ (its projection is also zero, $M = 0$); therefore, $l_x = l_y = l$, and the expansion is made in functions

$$\Phi_n^{ll}(\Omega) = \frac{1}{2^{l_x}} N_n^{ll} (\sin 2\alpha)^l P_n^{l+1/2,l+1/2}(\cos 2\alpha) \times \sum_{m_x} (llmm_y = -m|00) Y_{lm}(\theta_x, \varphi_x) Y_{l-m}(\theta_y, \varphi_y). \quad (9)$$

Here, $(l_x l_y m_x m_y | LM)$ are the Clebsch–Gordan coefficients; $P_n^{l+1/2,l+1/2}$ are the Jacobi polynomials of order n (n is an integer); the hypermomentum K is

$$K = 2n + 2l_x, \quad (10)$$

and the normalization coefficient is determined by the equation

$$N_n^l = \sqrt{\frac{2n!(2l + 2n + 2)(n + 2l + 1)!}{\Gamma\left(n + l + \frac{3}{2}\right)\Gamma\left(n + l + \frac{3}{2}\right)}}, \quad (11)$$

where $\Gamma(z)$ is the gamma function. Functions $\Phi_{K00}^{ll}(\Omega)$ (9) actually depend only on the angle α and the angle θ between the vectors $\vec{x}$ and $\vec{y}$:

$$\Phi_n^{ll}(\alpha, \theta) = \frac{1}{2^l} N_n^{ll} (\sin 2\alpha)^l \times P_n^{l+1/2,l+1/2}(\cos 2\alpha)\sqrt{\frac{2l+1}{2}} P_l(\cos\theta). \quad (12)$$

The wave function Ψ_0 of the ground state of the system consisting of two α-clusters and the neutron is a series with summation over l and n:

$$\Psi_0(\alpha, \theta, \rho) = \sum_{ln} \chi_n^l(\rho)\rho^{-5/2}(\sin\alpha\cos\alpha)^l \times N_n^l P_n^{l+1/2,l+1/2}(\cos 2\alpha)\sqrt{\frac{2l+1}{2}} P_l(\cos\theta), \quad (13)$$

in which the functions $\chi_n^l(\rho)$ are determined from the system of hyperradial equations

$$\frac{d^2}{d\rho^2}\chi_n^l(\rho) + \left[2Eb_0 - \frac{1}{\rho^2}(K + 3/2)(K + 5/2)\right]\chi_n^l(\rho) = 2b_0\sum_{n'l'}\tilde{U}_{nn'}^{l;l'}(\rho), \quad (14)$$

with the boundary conditions

$$\chi_n^l(0) = 0, \quad \chi_n^l(\rho) \to 0, \quad \rho \to \infty, \quad (15)$$

and the channel coupling matrix

$$\tilde{U}_{nn'}^{l;l'}(\rho) = \langle lln0|\tilde{U}|l'l'n'0\rangle. \quad (16)$$

Coupling matrix (16)

$$\tilde{U}_{n;n'}^{l;l'}(\rho) = \int d\Omega \Phi_{n'}^{l'l'*}\tilde{U}\Phi_n^{ll} = \int_0^{\pi/2} d\alpha\cos^2\alpha\sin^2\alpha \int_0^{\pi} d\theta\sin\theta\Phi_{n'}^{l'l'*}\tilde{U}\Phi_n^{ll} \quad (17)$$

with the potential energy of the system with pair interactions,

$$U = V_{\alpha-\alpha}(R) + V_{\alpha-n}\left(\left|\frac{1}{2}\vec{R} - \vec{r}\right|\right) + V_{\alpha-n}\left(\left|\frac{1}{2}R + \vec{r}\right|\right), \quad \tilde{U} = U/\varepsilon_0, \quad (18)$$

was calculated using Gaussian quadrature formulas of order from 32 to 80.

APPLICATION OF CUBIC SPLINES TO SOLVING HYPERRADIAL EQUATIONS

Cubic splines allow one not only to construct a smooth function based on its values f_i at grid nodes, but also to express the values of the second derivative $m_i = f''(x_i)$ at grid nodes through f_i:

$$Am = HF, \tag{19}$$

where F is the column of values f_i, and the explicit forms of the matrices A and H were given in Marchuk's monograph [6]. This provides a convenient opportunity to reduce the boundary-value differential problem to a matrix eigenvalue problem. The boundary-value problem for hyperradial equations (14) also reduces to the problem of eigenvalues and eigenvectors of a block matrix [4]:

$$BF = \lambda F, \quad B = -A^{-1}HF + WF, \qquad \lambda = \frac{2\mu}{\hbar^2}E, \tag{20}$$

where

$$W_{i,i} = 2b_0\tilde{U}^{l_x;l_x'}_{KK'}(\rho_i) + \frac{1}{\rho_i^2}(K+3/2)(K+5/2)\delta_{K;K'}\delta_{l_x;l_x'}, \tag{21}$$

$$A_{i,i} = I\frac{h_i + h_{i+1}}{3}, \quad A_{i,i+1} = A_{i+1,i} = I\frac{h_{i+1}}{6}, \tag{22}$$

$$H_{i+1,i} = H_{i,i+1} = I\frac{1}{h_{i+1}}, \qquad H_{i,i} = -I\left(\frac{1}{h_i} + \frac{1}{h_{i+1}}\right), \tag{23}$$

$$F_i = \chi_K^{l_x}(\rho_i), \quad i = 1,\ldots,n_p - 1, \tag{24}$$

and $h_i = \rho_i - \rho_{i-1}$, $i = 1,\ldots,n_p$, $\rho_0 = 0$, $\rho_{n_p} = \rho_{\max}$. In general, the method can be used on a nonuniform grid ρ_i; in this work, a uniform grid $\rho_i = ih$, $i = 0,\ldots,n_p$, was used. The eigenvalues and eigenvectors of the matrix in problem (20) were found by the QR and QL methods [9]; the calculations were carried out using the NVIDIA CUDA platform [10]. Some of the calculations were performed on a heterogeneous cluster of the Laboratory of Information Technologies, Joint Institute for Nuclear Research [11].

The interaction of an α particle with the neutron was described by the pseudopotential

$$V_{\alpha-n}(r) = -U_{n1}f(r,B_{n1},a_{n1}) + U_{n2}f(r,B_{n2},a_{n2}) - U_{n3}f(r,B_{n3},a_{n3})f(r,B_{n4},a_{n4}). \tag{25}$$

Pseudopotentials are used in metal physics to describe the interaction of valence electrons with atomic cores and to approximately calculate the outer part of the electron wave function outside the atomic core. Similarly, pseudopotential (25) was used in this work to calculate the outer part of the neutron wave function outside the inner part of the α particle, occupied by closely spaced pairs of protons and neutrons. Figure 1a presents the graph of pseudopotential (25). The following values of the parameters of potential (25) were proposed previously [4]:

$$U_{n1} = 64.8 \text{ MeV}, \quad B_{n1} = 1.95 \text{ fm}, \quad a_{n1} = 0.25 \text{ fm}, \tag{26}$$

$$U_{n2} = 55.8 \text{ MeV}, \quad B_{n2} = 1.22 \text{ fm}, \quad a_{n2} = 0.3 \text{ fm}, \tag{27}$$

$$U_{n3} = 107 \text{ MeV}, \quad B_{n3} = 0.9 \text{ fm}, \quad a_{n3} = 0.5 \text{ fm}, \quad B_{n4} = 2.7 \text{ fm}, \quad a_{n4} = 1 \text{ fm}. \tag{28}$$

The scattering of α-particles at low energies is described by the Ali–Bodmer potential [8] with the nuclear part in the form

$$V^{(N)}_{\alpha-\alpha}(r) = v_1\exp\left(-r^2/a_1^2\right) - v_2\exp\left(-r^2/a_2^2\right) \tag{29}$$

and the Coulomb part $V^{(C)}_{\alpha-\alpha}(r)$ approximated using the error function erf(x),

$$V^{(C)}_{\alpha-\alpha}(r) = a_C\,\mathrm{erf}\,(b_C r)/r, \tag{30}$$

where $b_C = 0.601$ fm^{-1} and $a_C = Z_\alpha^2 e^2/x_0 = 5.759$ MeV fm [8]. The values of the parameters of the nuclear part of the potential, which were determined from the condition that the theoretical and experimental values of the s-scattering phase are close, are the following [8]:

$$v_1 = 125 \text{ MeV}, \quad a_1^2 = 2.3409 \text{ fm}^2, \qquad v_2 = 30.18 \text{ MeV}, \quad a_2^2 = 8.1225 \text{ fm}^2. \tag{31}$$

Figure 1b presents the graph of the potential of interaction of α-particles in the Ali–Bodmer form

$$V_{\alpha-\alpha}(r) = V^{(N)}_{\alpha-\alpha}(r) + V^{(C)}_{\alpha-\alpha}(r). \tag{32}$$

The nuclear part of potential (32) has a strongly repulsive central part (core), which can be explained as a consequence of the averaged action of the repulsive core of the nucleon–nucleon interaction and the Pauli principle.

Generally speaking, the interaction of α-clusters within the stable ^{9}Be nucleus may differ from the interaction in collisions of α-particles, which lasts for a fairly short period of time (time of flight). To obtain greater possibilities for modifying the interaction, it is convenient to use the previously proposed form [4] with six parameters,

$$V^{(N)}_{\alpha-\alpha}(r) = -U_{\alpha1}f(r,B_{\alpha1},a_{\alpha1}) + U_{\alpha2}f(r,B_{\alpha2},a_{\alpha2}), \tag{33}$$

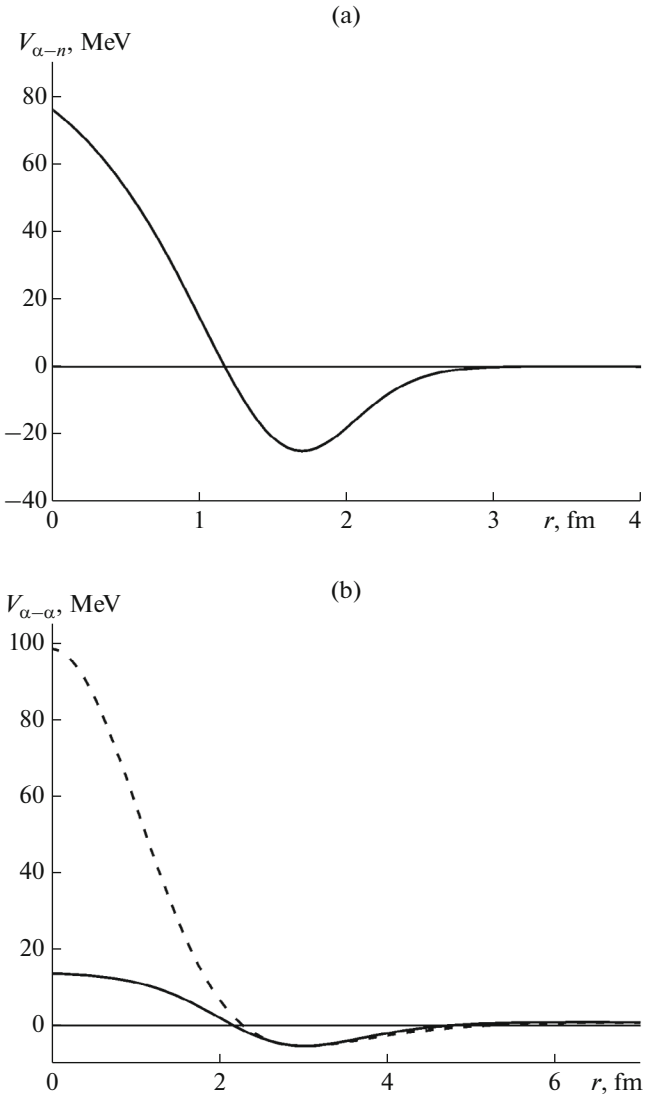

Fig. 1. Graphs of (a) the pseudopotential $V_{\alpha-n}(r)$ of interaction of an α-particle with a neutron and (b) the potential $V_{\alpha-\alpha}(r)$ of interaction of α-particles: Ali–Bodmer potential (29) (dashed curve) and potential (33) with parameters (42) and (43) (solid curve).

and function $f(r,B,a)$ of the Woods–Saxon type (Fermi distribution),

$$f(r,B,a) = \left[1 + \exp\left(\frac{r-B}{a}\right)\right]^{-1}, \tag{34}$$

instead of Gaussian exponentials in the Ali–Bodmer potential. During the calculations, the parameters of potential (33) were varied to ensure the closeness of the theoretical and experimental values of the energy E_0 of the ground state of the system $(\alpha + n + \alpha)$, which is equal to the energy of its decomposition into components with the opposite sign, $E_0 = -E_s$. The experimental value of E_s is equal to the neutron separation energy: $E_s = 1.66452$ MeV (see, e.g., [12]), since the ^{8}Be nucleus is unbound. The root-mean-square charge radius $\langle r_{Be}^2 \rangle$ of the system is determined by the root-mean-square charge radius of the charge distribution in the α-cluster, which was considered the same as that for the α-particle, $\langle r_{He}^2 \rangle$, and by the root-mean-square radius of the distribution of α-cluster centers $\langle r_\alpha^2 \rangle$:

$$\langle r_{Be}^2 \rangle = \langle r_\alpha^2 \rangle + \langle r_{He}^2 \rangle; \tag{35}$$

$$\langle r_\alpha^2 \rangle = \frac{\int_0^\infty R^2 dR \int_0^\infty r^2 dr \int_0^\pi |\Psi|^2 R_\alpha^2 \sin(\theta)\, d\theta}{\int_0^\infty R^2 dR \int_0^\infty r^2 dr \int_0^\pi |\Psi|^2 \sin(\theta)\, d\theta}, \tag{36}$$

where R_α is the distance between the α-particle and the center of mass of the system,

$$R_\alpha^2 = \left(\frac{1}{2}\vec{R} + \vec{r}\,\frac{1}{9}\right)^2 = \frac{1}{4}R^2 + \frac{1}{9}Rr\cos\theta + \frac{1}{81}r^2. \tag{37}$$

The calculations of the wave function Ψ_0 of the ground state allow one to find $\langle r_\alpha^2 \rangle$, and the root-mean-square charge radii of the ^{4}He and ^{9}Be nuclei are $\langle r_{He}^2 \rangle^{1/2} = 1.68$ fm and $\langle r_{Be}^2 \rangle^{1/2} = 2.52$ fm, respectively (see, e.g., [12]). Using the electric charge distribution $\rho_{He}(r)$ in the ^{4}He nucleus, one can calculate the electric charge distribution in the ^{9}Be nucleus. Figures 2a and 2b show the experimentally measured electric charge distributions $\rho(r)$ in the ^{4}He and ^{9}Be nuclei, respectively [13, 14], satisfying the normalization condition to the atomic number Z of the nucleus:

$$Z = \int \rho(r) d^3 r. \tag{38}$$

In Fig. 2a, the charge distribution in the ^{4}He nucleus is approximated by the function

$$\rho_{He}(r) = \frac{\rho_1}{1 + 2\exp\left(-\frac{b}{a}\right)\left[\cosh\left(\frac{r}{a}\right) - 1\right]} + \rho_2 \exp\left(-\frac{(r-c)^2}{d^2}\right), \tag{39}$$

where

$$\rho_1 = 0.112 \text{ fm}^{-3}, \quad \rho_2 = 0.0073 \text{ fm}^{-3}, \tag{40}$$

$$a = 0.367 \text{ fm}, \quad b = 1.32 \text{ fm}, \quad c = 0.762 \text{ fm}, \quad d = 0.5 \text{ fm}. \tag{41}$$

The quantities E_0, $\langle r_\alpha^2 \rangle^{1/2}$, $\langle r_{Be}^2 \rangle^{1/2}$, and the electric charge distribution in the ^{9}Be nucleus were calculated for Ali–Bodmer potential (29) with fixed parameters and for potential (33) with varied parameters. Quite a

good agreement with experimental data was obtained at the following parameter values:

$$U_{\alpha 1} = 17.3 \text{ MeV}, \quad U_{\alpha 2} = 27.25 \text{ MeV}. \tag{42}$$

$$B_{\alpha 1} = 3.3 \text{ fm}, \quad B_{\alpha 2} = 2.1 \text{ fm}, \quad a_{\alpha 1} = 0.58 \text{ fm}, \quad a_{\alpha 2} = 0.48 \text{ fm}. \tag{43}$$

Figure 1b presents the graph of the potential $V^{(N)}_{\alpha-\alpha}(r)$ of interaction of α-clusters in the ^{9}Be nucleus. Figure 2b shows the charge distributions $\rho(r)$ in the ^{9}Be nucleus obtained for potential (33) and Ali–Bodmer potential (29):

$$\rho(r) = \int n(r_1)\rho_{\text{He}}(|\vec{r} - \vec{r}_1|)dr_1^3. \tag{44}$$

Here, $n(r_1)$ is the radial (r_1) distribution function of centers of α-particles, normalized by the condition

$$\int n(r)d^3r = 2, \tag{45}$$

which is shown in Fig. 2c for potential (33) and Ali–Bodmer potential (29). The function $n(r_1)$ is determined by the expression

$$n(r_1) = 2\int dRR^2 \int drr^2 \int_0^\pi d\theta \sin\theta |\Psi_0(R,r,\theta)|^2 \times \delta(r_1 - R_\alpha(R,r,\theta)), \tag{46}$$

where $\delta(r)$ is the Dirac delta function, the wave function $\Psi_0(R,r,\theta)$ depending on the magnitudes of the Jacobi vectors and the angle between them, normalized by the condition

$$\int dRR^2 \int drr^2 \int_0^\pi d\theta \sin\theta |\Psi_0(R,r,\theta)|^2 = 1, \tag{47}$$

and the domain of integration over variables R, r is specified by the range of hyperradius values, $0 < \rho(R,r) \le \rho_{\max}$. In numerical calculations, the Dirac delta function was replaced by the step function

$$\delta(r) = \begin{cases} \dfrac{1}{\Delta r}, \text{ at } |r| \le \dfrac{\Delta r}{2}, \\ 0, \text{ at } |r| > \dfrac{\Delta r}{2}. \end{cases} \tag{48}$$

Table 1 presents the results of calculation of the energy E_0 of the ground state of the system $(\alpha + n + \alpha)$ and the root-mean-square radii $\langle r_\alpha^2 \rangle^{1/2}$ and $\langle r_{\text{Be}}^2 \rangle^{1/2}$ for Ali–Bodmer potential (29) and for potential (33) with parameters (42) and (43). Figure 2b shows that using the Ali–Bodmer potential does not give the correct charge distribution and leads to the values E_0 and $\langle r_{\text{Be}}^2 \rangle^{1/2}$ that noticeably differ from the experimental ones. Using potential (33), a better agreement was achieved with experimental data for energy and charge distribution. The slight excess of the value for the root-

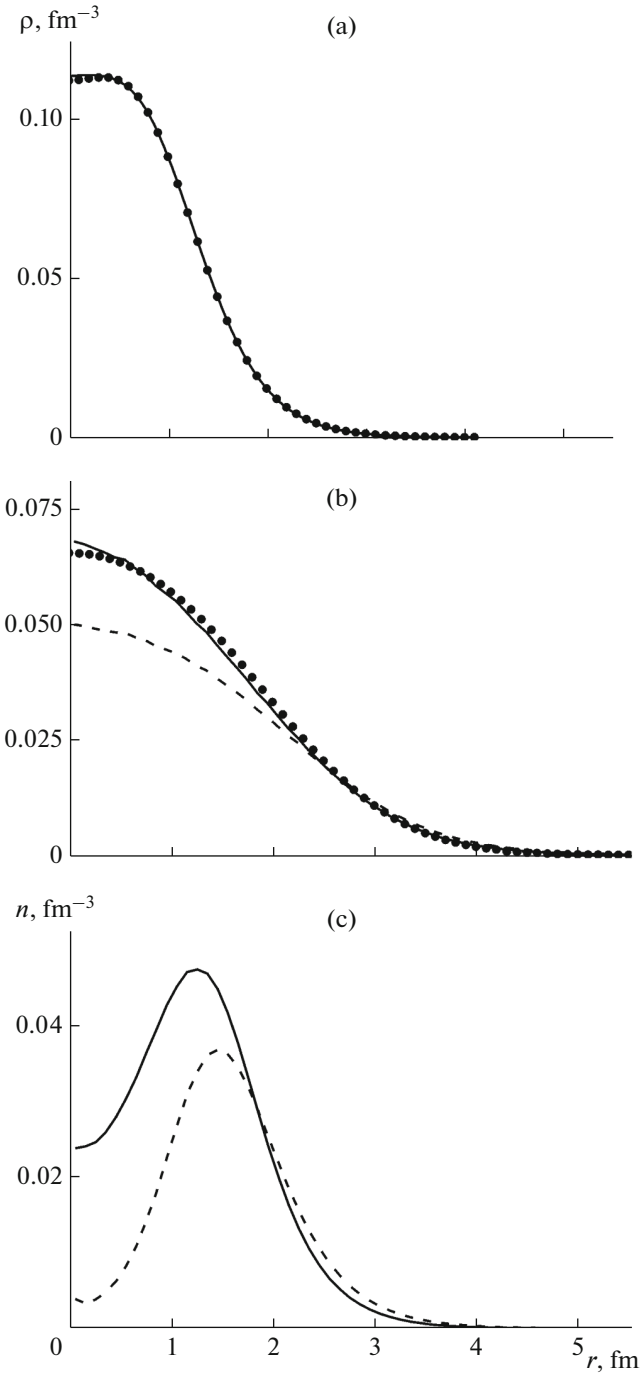

Fig. 2. (a) Density $\rho_{\text{He}}(r)$ of distribution of electric charge (in units of elementary charge) in the ^{4}He nucleus: the points represent the experimental data [13]; the curve, their approximation (39). (b) Density $\rho(r)$ of distribution of electric charge (in units of elementary charge) in the ^{9}Be nucleus: the points represent the experimental data [14]; the curves, the calculated potentials $V_{\alpha-\alpha}(r)$ of interaction of α-particles (Ali–Bodmer potential (29), dashed curve) and interaction of α-clusters (potential (33), solid curve). (c) Radial (r_1) distribution functions of centers of α-clusters for potential (33) (solid curve) and Ali–Bodmer potential (29) (dashed curve).

Table 1. Calculated values of the energy E_0 of the ground state of the system ($\alpha + n + \alpha$) and the root-mean-square radii $\langle r_\alpha^2 \rangle^{1/2}$ and $\langle r_{Be}^2 \rangle^{1/2}$ at $\rho_{max} = 30$ fm and $h = 0.2$ fm for Ali–Bodmer potential (29) and potential (33) with parameters (42) and (43); the experimental values are $E_0 = -1.664$ MeV and $\langle r_{Be}^2 \rangle = 2.52$ fm (see, e.g, [12])

		E_0, MeV		$\langle r_\alpha^2 \rangle^{1/2}$, fm		$\langle r_{Be}^2 \rangle$, fm	
n_{max}	l_{max}	$V_{\alpha-\alpha}^{(N)}$ (29)	$V_{\alpha-\alpha}^{(N)}$ (33)	$V_{\alpha-\alpha}^{(N)}$ (29)	$V_{\alpha-\alpha}^{(N)}$ (33)	$V_{\alpha-\alpha}^{(N)}$ (29)	$V_{\alpha-\alpha}^{(N)}$ (33)
2	2	−0.5814	−0.9979	2.3260	2.0577	2.7875	2.6466
4	4	−1.0813	−1.4824	2.2333	2.0	2.7854	2.6020
6	6	−1.2378	−1.6135	2.2308	2.0079	2.7834	2.6081
8	8	−1.2815	−1.6471	2.2418	2.0160	2.7922	2.6144
10	10	−1.2949	−1.6562	2.2502	2.0237	2.7989	2.6203
12	12	−1.2993	−1.6591	2.2530	2.0266	2.8012	2.6225

Table 2. Energies (MeV) of the ground state of a system consisting of two α-clusters and a neutron (or energies of separation of a neutron from the ^{9}Be nucleus) at various steps h, various maximum values n_{max} and l_{max} of quantum numbers, and $\rho_{max} = 30$ fm

n_{max}	l_{max}	h, fm		
		1	0.5	0.2
4	4	−1.4160	−1.4661	−1.4824
8	8	−1.580	−1.6307	−1.6471
12	12	−1.5925	−1.6429	−1.6591
16	16	−1.5939	−1.6442	−1.6602

mean-square charge radius can be explained by the use of the charge distribution in the free ^{4}He nucleus, which differs from the charge distribution in α-clusters of the ^{9}Be nucleus. In contrast to the Ali–Bodmer potential, more accurate form (33) of the interaction of α-clusters in the ^{9}Be nucleus has a softer repulsive core for colliding α-particles in the region of small distances between the centers of α-clusters, $r \le 2$ fm. This allows one to judge the modification of α-clusters in the ^{9}Be nucleus in comparison with free α-particles, in particular, their polarization, deformation, and mutual overlap.

The structure of the ^{9}Be nucleus is provided by the probability density maps for the three-body wave function in Fig. 3, which shows the probability density $|\Psi_0|^2$ at two values $\theta = \pi/2$ and $\theta = 0$ of the angle between the Jacobi vectors in combination with the potential relief. The correspondence between the probability density and the potential relief, in particular, the presence of local maxima of $|\Psi_0|^2$ near local minima of the potential energy indicates the correctness of the calculations performed. The most probable is a three-body configuration with a valence neutron between α-particles at a distance between their centers of $x = |\vec{r}_{\alpha_2} - \vec{r}_{\alpha_1}| \approx 3$ fm, which corresponds to the vicinity of the potential minimum $V_{\alpha-\alpha}(r)$ (Fig. 1b). The probability density distributions shown in Fig. 3 are consistent with ideas about the structure of the ^{9}Be nucleus as a nuclear molecule consisting of two α-particles (α-clusters) and an outer (valence) neutron [3, 4]. The results obtained agree with the published maps of the relative positions of α-clusters and neutrons [3, 4] and refine the spatial parameters of this nuclear molecule.

The use of spline interpolation allows one to construct smooth solutions throughout the range (ρ_{min}, ρ_{max}) even at a not very small grid step h. The results of the numerical solution of hyperradial equations using cubic spline interpolation are shown in Fig. 4 at $h = 1$ fm. Tables 1 and 2 demonstrate the convergence of the results to the accurate value of the energy of separation of a neutron from the ^{9}Be nucleus, which is close to the experimental value $E_0 = -1.664$ MeV (see, e.g., [12]).

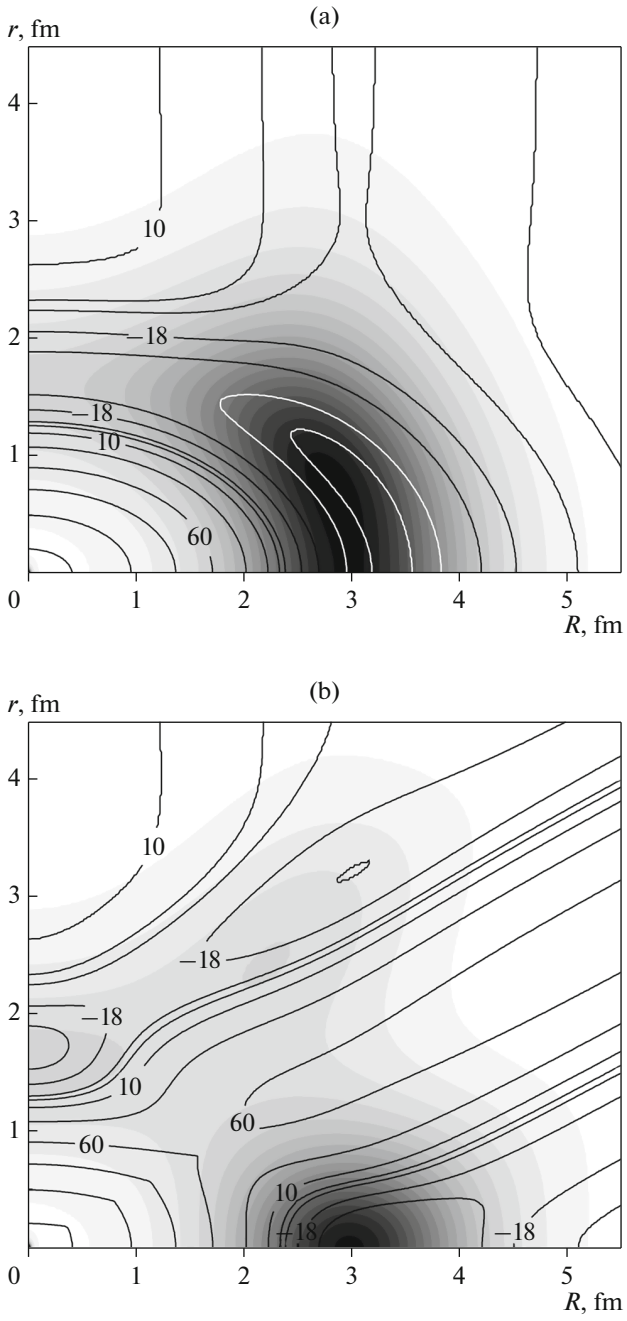

Fig. 3. Probability density $|\Psi_0(R,r,\cos\theta)|^2$ (linear gray-scale) at two values (a) $\theta = \pi/2$ and (b) $\theta = 0$ of the angle between the Jacobi vectors $\vec{R},\vec{r}$, calculated at $n_{max} = 14$, $L_{max} = 14$, $\rho_{max} = 30$ fm, and $h = 0.2$ fm together with the potential energy lines of the system. The numbers in some lines are the corresponding values of potential energy U (18) of the system.

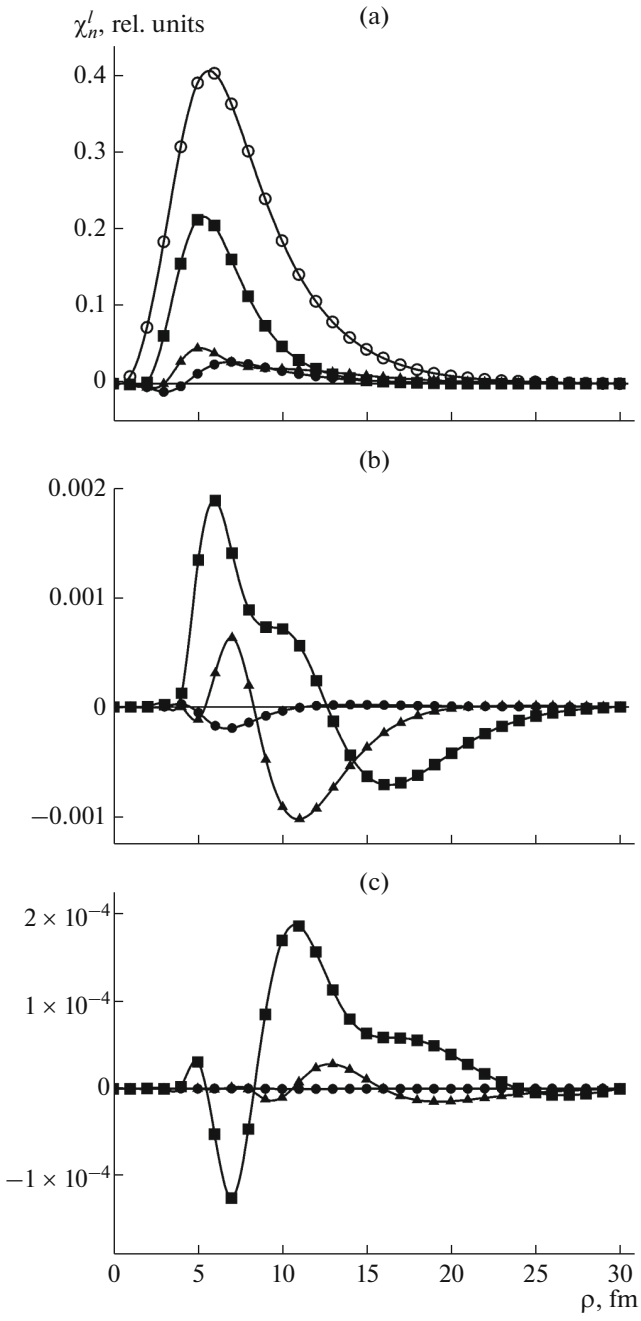

Fig. 4. Examples of solutions to the system of hyperradial equations (14) at $n_{max} = 16$, $L_{max} = 16$, $\rho_{max} = 30$ fm, and $h = 1$ fm. The points represent the values of the function $\chi^l_n(\rho)$ at grid nodes: (a) (○) $n = l = 0$, (■) $n = 1$, $l = 0$, (●) $n = 0$, $l = 2$, and (▲) $n = 1$, $l = 2$; (b) (■) $n = 8$, $l = 0$, (●) $n = 0$, $l = 8$, and (▲) $n = l = 8$; and (c) (■) $n = 16$, $l = 0$, (●) $n = 0$, $l = 16$, and (▲) $n = 16$, $l = 16$. The curve represents the results of interpolation by cubic splines between nodes.

CONCLUSIONS

The proposed method for solving hyperradial equations can be useful for studying three-body systems in nuclear and atomic physics. For the ^{9}Be nucleus, this method made it possible to calculate the neutron separation energy, root-mean-square charge radius, and charge distribution and obtain agreement with experimental values.

ACKNOWLEDGMENTS

We thank the team of the heterogeneous cluster of the Laboratory of Information Technologies, Joint Institute for Nuclear Research, for their assistance in performing laborious computer calculations.

FUNDING

This work was supported by ongoing institutional funding. No additional grants to carry out or direct this particular research were obtained.

CONFLICT OF INTEREST

The authors of this work declare that they have no conflicts of interest.

REFERENCES

1. von Oertzen, W., Freer, M., and Kanada En'yo, Y., *Phys. Rep.*, 2006, vol. 432, p. 43.
2. Freer, M., *Rep. Progr. Phys.*, 2007, vol. 70, p. 2149.
3. Samarin, V.V., *Bull. Russ. Acad. Sci.: Phys.*, 2020, vol. 84, p. 981.
4. Samarin, V.V., *Eur. Phys. J. A*, 2022, vol. 58, p. 117.
5. Dzhibuti, R.I. and Shitikova, K.V., *Metod gipersfericheskikh funktsii v atomnoi i yadernoi fizike* (Method of Hyperspherical Functions in Atomic and Nuclear Physics), Moscow: Energoatomizdat, 1993.
6. Marchuk, G.I., *Metody vychislitel'noi matematiki* (Methods of Computational Mathematics), Moscow: Nauka, 1980.
7. Blokhintsev, D.I., *Osnovy kvantovoi mekhaniki* (Fundamentals of Quantum Mechanics), Moscow: Nauka, 1976.
8. Ali, S. and Bodmer, A.R., *Nucl. Phys. A*, 1966, vol. 80, p. 99.
9. Wilkinson, J.H., and Reinsch, C., *Handbook for Automatic Computation: Linear Algebra*, Berlin: Springer, 1975.
10. Sanders, J. and Kandrot, E., *CUDA by Example: An Introduction to General-Purpose GPU Programming*, New York: Addison-Wesley, 2010.
11. http://hybrilit.jinr.ru.
12. http://nrv.jinr.ru.
13. Jansen, I.A., Peerdeman, R.Th., and de Vries, C., *Nucl. Phys. A*, 1972, vol. 188, p. 337.
14. Sick, I., *Phys. Lett. B*, 1982, vol. 116, p. 212.